J|A|C|S ARTICLES

Published on Web 06/16/2010

Structure of a GPCR Ligand in Its Receptor-Bound State: Leukotriene B4 Adopts a Highly Constrained Conformation When Associated to Human BLT2

Laurent J. Catoire,*,† Marjorie Damian,‡ Fabrice Giusti,† Aimée Martin,‡ Carine van Heijenoort,¶ Jean-Luc Popot,† Éric Guittet,¶ and Jean-Louis Banères*,‡

Laboratoire de Biologie Physico-Chimique des Protéines Membranaires, UMR 7099, CNRS/ Université Paris-7, Institut de Biologie Physico-Chimique (FRC 550), 13 rue Pierre et Marie Curie, F-75005 Paris, France, Institut des Biomolécules Max Mousseron, UMR 5247 CNRS, Université Montpellier 1 and Université Montpellier 2, 15 Avenue C. Flahault, F-34093 Montpellier, France, and Centre de Recherche de Gif, Laboratoire de Chimie et Biologie Structurales, ICSN, UPR 2301, CNRS, F-91198 Gif-sur-Yvette, France

Received March 5, 2010; E-mail: laurent.catoire@ibpc.fr; jean-louis.baneres@univ-montp1.fr

Abstract: G protein-coupled receptors (GPCRs) are key players in signal recognition and cell communication and are among the most important targets for drug development. Direct structural information on the conformation of GPCR ligands bound to their receptors is scarce. Using a leukotriene receptor, BLT2, expressed under a perdeuterated form in *Escherichia coli*, purified in milligram amounts, and folded to its native state using amphipols, we have solved, by ^{1}H NMR, the structure of receptor-bound leukotriene B4 (LTB4). Upon binding, LTB4 adopts a highly constrained seahorse conformation, at variance with the free state, where it explores a wide range of conformations. This structure provides an experimentally determined template of a pro-inflammatory compound for further pharmacological studies. The novel approach used for its determination could prove powerful to investigate ligand binding to GPCRs and membrane proteins in general.

Introduction

G protein-coupled receptors (GPCRs) are integral membrane proteins involved in many important signal transduction processes, including the mediation of hormonal activity and cell-to-cell communication.[1] Despite their exceptional clinical relevance, only a very limited set of high-resolution GPCR structures have been established to date.[2−7] Direct structural information regarding ligand binding and the mechanisms of GPCR activation is also very limited.[8] A detailed knowledge of the structure adopted by ligands upon binding to their receptors would considerably help in developing original compounds with potential therapeutic applications, as well as unraveling how the transfer of information from the exterior to the interior of the cell takes place. Various types of lipids have been reported to activate GPCRs.[9] Among those are leukotrienes (LTs), a family of endogenous metabolites of arachidonic acid biosynthesized via the lipoxygenase pathway.[10,11] LTs include potent bronchoconstrictors that play important roles in immediate hypersensitivity reactions and act as mediators of inflammatory process, while other members of the family are potent chemotactic agents. Like prostaglandins and other LTs, leukotriene B4 (5*S*,12*R*-dihydroxy-6*Z*,8*E*,10*E*,14*Z*-eicosatetraenoic acid; LTB4) belongs to the family of eicosanoids. It is characterized by a triene motif and the presence of two hydroxyl groups and an acidic function (Figure 1a). LTB4 is known to activate both high- and low-affinity receptors, respectively BLT1[12] and BLT2,[13−16] which are involved in a large panel of

† Laboratoire de Biologie Physico-Chimique des Protéines Membranaires, UMR 7099.

‡ Institut des Biomolécules Max Mousseron, UMR 5247.

¶ Centre de Recherche de Gif, Laboratoire de Chimie et Biologie Structurales, ICSN, UPR 2301.

(1) Bockaert, J.; Claeysen, S.; Bécamel, C.; Pinloche, S.; Dumuis, A. *Int. Rev. Cytol.* **2002**, *212*, 63–132.
(2) Palczewski, K.; Kumasaka, T.; Hori, T.; Behnke, C. A.; Motoshima, H.; Fox, B. A.; Le Trong, I.; Teller, D. C.; Okada, T.; Stenkamp, R. E.; Yamamoto, M.; Miyano, M. *Science* **2000**, *289*, 739–745.
(3) Cherezov, V.; Rosenbaum, D. M.; Hanson, M. A.; Rasmussen, S. G.; Thian, F. S.; Kobilka, T. S.; Choi, H. J.; Kuhn, P.; Weis, W. I.; Kobilka, B. K.; Stevens, R. C. *Science* **2007**, *318*, 1258–1265.
(4) Rasmussen, S. G.; Choi, H. J.; Rosenbaum, D. M.; Kobilka, T. S.; Thian, F. S.; Edwards, P. C.; Burghammer, M.; Ratnala, V. R.; Sanishvili, R.; Fischetti, R. F.; Schertler, G. F.; Weis, W. I.; Kobilka, B. K. *Nature* **2007**, *450*, 383–387.
(5) Warne, T.; Serrano-Vega, M. J.; Baker, J. G.; Moukhametzianov, R.; Edwards, P. C.; Henderson, R.; Leslie, A. G.; Tate, C. G.; Schertler, G. F. *Nature* **2008**, *454*, 486–491.
(6) Park, J. H.; Scheerer, P.; Hofmann, K. P.; Choe, H. W.; Ernst, O. P. *Nature* **2008**, *454*, 183–187.
(7) Jaakola, V. P.; Griffith, M. T.; Hanson, M. A.; Cherezov, V.; Chien, E. Y.; Lane, J. R.; Ijzerman, A. P.; Stevens, R. C. *Science* **2008**, *322*, 1211–1217.
(8) Bokoch, M. P.; et al. *Nature* **2010**, *463*, 108–112.
(9) Okuno, T.; Yokomizo, T.; Mitano, M.; Shimizu, T. *J. Biol. Chem.* **2005**, *280*, 32049–32052.
(10) Borgeat, P.; Hamberg, M.; Samuelsson, B. *J. Biol. Chem.* **1976**, *251*, 7816–7820.
(11) Izumi, T.; Yokomizo, T.; Obinata, H.; Ogasawara, H.; Shimizu, T. *J. Biochem.* **2002**, *132*, 1–6.
(12) Yokomizo, T.; Izumi, T.; Chang, K.; Takuwa, Y.; Shimizu, T. *Nature* **1997**, *387*, 620–624.
(13) Kamohara, M.; Takasaki, J.; Matsumoto, M.; Saito, T.; Ohishi, T.; Ishii, H.; Furuichi, K. *J. Biol. Chem.* **2000**, *275*, 27000–27004.

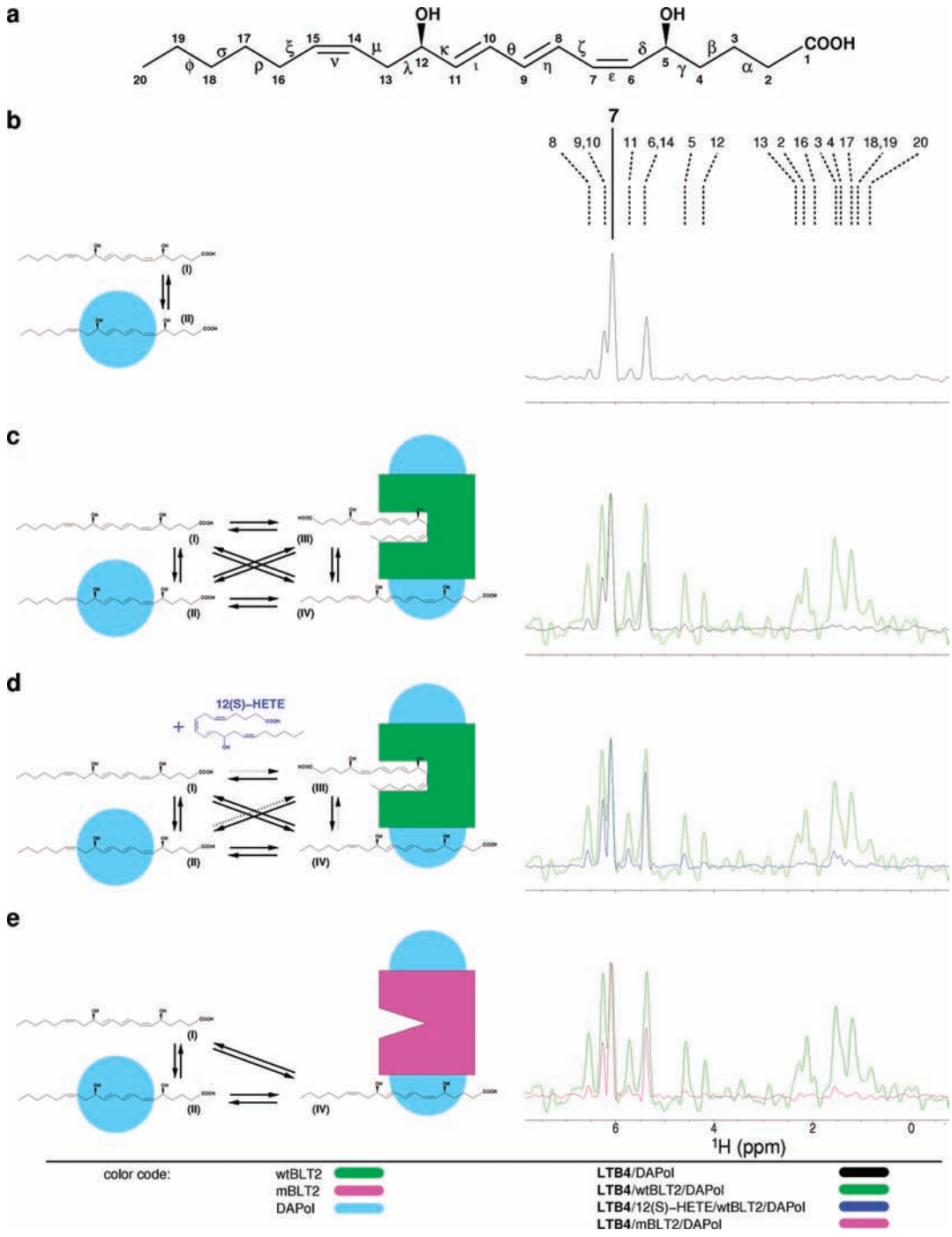

Figure 1. Illustration of the olefinic/aliphatic ^{1}H dipolar interactions for LTB4 in the presence of different partners in solution. (a) Chemical structure of LTB4 (Greek letters refer to the dihedral angles described in Supporting Information (SI) Figure 16). (b) LTB4 in the presence of free DAPol. Schematic view (*left*) of the two coexisting states, I (free), and II (associated to particles of DAPol), black arrows symbolizing the chemical exchange. On the *right*, 1D column extracted from a 2D NOESY experiment (τ_m = 500 ms) at the Larmor frequency of proton H7 (see also Figure 3a). The ^{1}H assignments are indicated above the spectrum; the diagonal peak is indicated by a solid line. (c) LTB4 in the presence of perdeuterated wild-type BLT2 receptor (u-^{2}H-wtBLT2) complexed by DAPol. The scheme on the *left* describes four putative states of LTB4. In addition to the states shown in (b), states III and IV represent, respectively, LTB4 interacting with the high affinity site of the receptor and with either a low affinity site and/or the belt of DAPol. On the *right*, 1D column extracted from a 2D NOESY spectrum of LTB4 in the presence of wild-type receptor (in *green*), compared to a column extracted at the same frequency from the 2D NOESY spectrum obtained under the conditions shown in (b). (d) Same as in (c), but in the presence of the LTB4 competitor 12(*S*)-HETE (HETE/LTB4 molar ratio = 9:1, extracted column in *blue*). Dotted arrows symbolize a lower probability of exchange, as compared to solid arrows. (e) Same as in (c) but with a mutant receptor (u-^{2}H-mBLT2) (extracted column in *magenta*). All the columns have been normalized with respect to the diagonal peak.

inflammatory diseases and allergic responses.[11] BLT2 is less specific for LTB4 than BLT1 and recognizes a wide range of ligands.[9]

In the present work, we have investigated by ^{1}H NMR spectroscopy the structure of LTB4 bound to human BLT2. To produce BLT2, we have overexpressed a recombinant, perdeuterated receptor in *Escherichia coli*, targeted it to inclusion bodies, and purified it in SDS solution under an inactive form. The receptor was then folded to its native state by a highly efficient procedure[17] that resorts to polymeric surfactants called

amphipols (APols),[18−20] used here in a partially deuterated form.[21] Proton−proton distance measurements indicate that BLT2-bound LTB4 adopts a highly constrained conformation, quite distinct from the collection of structures that is populated when the ligand is free in solution. These data should prove useful for the development of anti-inflammatory compounds. More generally, this study validates a novel, possibly widely applicable approach to investigating the fundamental question of ligand binding to GPCRs and membrane proteins in general.

Material and Methods

Eicosanoid Preparation. Eicosanoids LTB4 and 12(*S*)-HETE were obtained from Cayman Chemical, Ann Arbor, MI, U.S.A., as ethanolic solutions. The ethanol was evaporated under vacuum. The eicosanoids were dissolved in D_2O ($^2H \geq 99.9\%$; Eurisotop, Saclay, France) and lyophilized before use. The stability of the eicosanoids was checked by NMR after each run of NMR measurements.

Synthesis of DAPol. Partially deuterated APol A8-35 (DAPol, see Supporting Information (SI) Figure 1) was obtained by grafting deuterated octylamine and isopropylamine groups onto a hydrogenated poly(acrylic acid) precursor.[21]

Site-Directed Mutagenesis. All mutations were introduced in the wild-type BLT2 receptor by PCR-mediated mutagenesis using the QuickChange multisite-directed mutagenesis kit (Stratagene) and the wild-type BLT2 construct as a template. Mutations were confirmed by nucleotide sequencing.

Overexpression, Purification, and Folding of Human Wild-Type and Mutant BLT2 Receptors. Perdeuterated wild-type and mutant human BLT2 receptors, respectively wtBLT2 and mBLT2, were overexpressed in Rosetta(DE3) *Escherichia coli* strain as fusions with an N-terminal domain of the α subunit of integrin $\alpha_5\beta_1$. D_2O-based minimal growth media ($^2H > 99\%$) with 2 $g \cdot L^{-1}$ of ^2H-D-glucose ($^2H > 97\%$, EURISO-TOP) was used. Purification of inclusion bodies (in H_2O solutions) and folding of the receptors were similar to procedures already described.[17]

NMR Sample Preparation. The following NMR samples were prepared: uniformly ^2H-labeled wtBLT2 and mBLT2 (u-^2H-wtBLT2 and u-^2H-mBLT2) in complex with DAPol in a 100% D_2O solution (HEPES/NaOH buffer, pH 8). NMR buffer solution is 50 mM ^2H-HEPES(d_{18})(CDN isotopes)/NaOH, 100 mM NaCl, 1 mM ^2H-EDTA(d_{16}) (CDN isotopes), 0.02% NaN_3. The final concentration of the NMR sample was 16.7 μM for u-^2H-wtBLT2 and 17.9 μM for u-^2H-mBLT2, with receptor/DAPol ratio of 1:5 (w/w). Lyophilized LTB4 was directly solubilized with the receptor NMR sample with a LTB4/receptor molar ratio of 8.6:1 for both samples ([LTB4] ≃ 140 μM with wtBLT2 and ∼150 μM with mBLT2 samples). A competition experiment was carried out by adding 12(*S*)-HETE to u-^2H-wtBLT2 (16.6 μM) in the presence of LTB4 (LTB4/wtBLT2 molar ratio ≃9:1). The HETE/LTB4 molar ratios were equal to 1.6:1, 4.2:1, and 9.0:1 (checked with a 1D ^1H NMR spectrum). Two control samples were also prepared: LTB4 free in solution or in the presence of DAPol alone. Both samples were prepared in the NMR buffer and with LTB4 and DAPol concentrations identical to those employed in receptor-containing samples.

NMR Spectroscopy. All NMR experiments were carried out at 25 °C (see the time-dependent stability of A8-35-folded BLT2 at this temperature in SI Figure 2) and 600 MHz on a Bruker Avance spectrometer equipped with a cryoprobe. The following parameters were used for 2D NOESY experiments, which were carried out at four different mixing times (τ_m = 50, 100, 200, 500 ms): data size = 256(t_1) × 8,192(t_2) complex points, $t_{1_{max}}$ = 32 ms, $t_{2_{max}}$ = 511 ms, 256 acquisitions per increment, experiment time = 28.2−36.4 h. ^1H chemical shifts are referenced to H_2O (calibrated at 4.7 ppm at 25 °C). Chemical shift assignments are based on COSY spectra (SI Figure 3). Data processing was performed with NMRPipe software,[22] and spectra were analyzed with NMRView.[23]

Structure Calculation. The LTB4 pdb file was produced with AMBER 9.[24] Parameter and topology files were generated with XPLO2D (version 3.3.2).[25] Structure calculations were performed with the program ARIA[26] associated to CNS[27] using the standard protocol. Calculations were based on four sets of NOE data corresponding to four distinct τ_m (SI Figure 4). A full relaxation matrix treatment of NOE data has been applied in ARIA/CNS to take into account indirect $^1H-^1H$ cross-relaxation pathways.[28,29] The kinetics of chemical exchange has not been incorporated in the analysis of NOEs with ARIA. In parallel, back ARIA/CNS-independent calculations with TRNOE software[30] were carried out to confirm that the evolution of the NOEs as a function of the mixing time is compatible with the slow-intermediate chemical exchange observed (SI Figure 5). At a fixed mixing time, when some nonspecific intraolefinic NOE cross-peaks appeared (≡ LTB4 cross-peaks observed in the presence of surfactant only or in that of the mutant receptor, mostly at $\tau_m \geq 200$ ms, SI Figure 6), they were excluded from the structure calculation. The structures were drawn using the open-source software PyMOL.[31]

Results

Free LTB4 in Solution or in the Presence of Surfactant. An earlier conformational analysis by NMR of LTB4 in solution indicated that this compound adopts an elongated structure with a planar triene motif (carbon atoms C5 to C12), the remainder of the molecule being flexible, with coexistence of various rotamers.[32] LTB4 is a fatty acid molecule and, as other amphiphiles, is likely to interact with lipids or surfactants. In the presence of partially deuterated amphipol A8-35[18,21] (SI Figure 1; hereafter referred to as DAPol), slight variations in chemical shift indeed can be observed (SI Figures 7 and 8b and Tables 1,2). Two-dimensional (2D) nuclear Overhauser (NOE) spectroscopy[33] (NOESY) spectra recorded at several mixing time (τ_m) intervals, at concentrations of LTB4 and

(14) Tryselius, Y.; Nilsson, N. E.; Kotarsky, K.; Olde, B.; Owman, C. *Biochem. Biophys. Res. Commun.* **2000**, *274*, 377–382.
(15) Wang, S.; Gustafson, E.; Pang, L.; Qiao, X.; Behan, J.; Maguire, M.; Bayne, M.; Laz, T. *J. Biol. Chem.* **2000**, *275*, 40686–40694.
(16) Yokomizo, T.; Kato, K.; Terawaki, K.; Izumi, T.; Shimizu, T. *J. Exp. Med.* **2000**, *192*, 421–432.
(17) Dahmane, T.; Damian, M.; Mary, S.; Popot, J.-L.; Banères, J.-L. *Biochemistry* **2009**, *48*, 6516–6521.
(18) Tribet, C.; Audebert, R.; Popot, J.-L. *Proc. Natl. Acad. Sci. U.S.A.* **1996**, *93*, 15047–15050.
(19) Popot, J.-L.; et al. *Cell. Mol. Life Sci.* **2003**, *60*, 1559–1574.
(20) Popot, J.-L. *Annu. Rev. Biochem.* **2010**, *79*, 737−775.
(21) Gohon, Y.; Pavlov, G.; Timmins, P.; Tribet, C.; Popot, J.-L.; Ebel, C. *Anal. Biochem.* **2004**, *334*, 318–334.
(22) Delaglio, F.; Grzesiek, S.; Vuister, G. W.; Zhu, G.; Pfeifer, J.; Bax, A. *J. Biomol. NMR* **1995**, *6*, 277–293.
(23) Johnson, B. A.; Blevins, R. A. *J. Biomol. NMR* **1994**, *4*, 603–614.
(24) Pearlman, D. A.; Case, D. A.; Caldwell, J. W.; Ross, W. S.; Cheatham, T. E.; DeBolt, S.; Ferguson, D.; Seibel, G.; Kollman, P. *Comput. Phys. Commun.* **1995**, *91*, 1–41.
(25) Kleywegt, G. J.; Jones, T. A. *Methods Enzymol.* **1997**, *277*, 208–230.
(26) Rieping, W.; Habeck, M.; Bardiaux, B.; Bernard, A.; Malliavin, T. E.; Nilges, M. *Bioinformatics* **2007**, *23*, 381–382.
(27) Brünger, A. T.; Adams, P. D.; Clore, G. M.; DeLano, W. L.; Gros, P.; Grosse-Kunstleve, R. W.; Jiang, J. S.; Kuszewski, J.; Nilges, M.; Pannu, N. S.; Read, R. J.; Rice, L. M.; Simonson, T.; Warren, G. L. *Acta Crystallogr., Sect. D: Biol. Crystallogr.* **1998**, *54*, 905–921.
(28) Bloembergen, N. *Physica* **1949**, *15*, 386–426.
(29) Linge, J. P.; Habeck, M.; Rieping, W.; Nilges, M. *J. Magn. Reson.* **2004**, *167*, 334–342.
(30) London, R. E.; Perlman, M. E.; Davis, D. G. *J. Magn. Reson.* **1992**, *97*, 79–98.
(31) DeLano, W. L. *The PyMOL Molecular Graphics System*; DeLano Scientific LLC: Palo Alto, CA, 2008.
(32) Sugiura, M.; Beierbeck, H.; Bélanger, P. C.; Kotovych, G. *J. Am. Chem. Soc.* **1984**, *106*, 4021–4025.
(33) Kumar, A.; Ernst, R. R.; Wüthrich, K. *Biochem. Biophys. Res. Commun.* **1980**, *95*, 1–6.

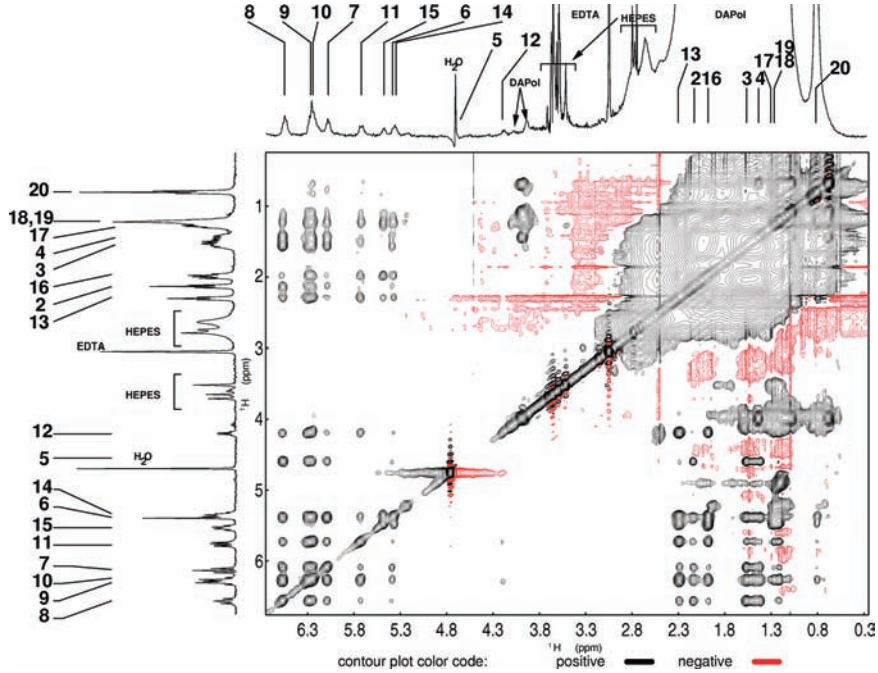

Figure 2. Dipolar interactions in the LTB4/u-^{2}H-wtBLT2/DAPol sample observed in a 2D NOESY spectrum (τ_m = 0.5 s, ν_H = 600 MHz, 25 °C). The corresponding 1D ^{1}H spectrum is shown above the 2D spectrum. In order to help in the identification of cross-peaks, the 1D spectrum of free LTB4 in solution is displayed on the left side. Numbers refer to the protons annotated on the LTB4 chemical structure in Figure 1a.

DAPol equivalent to those to be used in presence of the receptor, feature intense NOE cross-peaks between olefinic protons (5.2−6.7 ppm chemical shift range, e.g. Figure 1b), as well as between olefinic protons and the two protons that belong to a chiral center, namely H5 and H12. A few weak NOEs between olefinic and aliphatic protons (0.5−2.5 ppm chemical shift range) can also be observed, but exclusively at long τ_m (∼500 ms) (*vide infra* Figure 3). However, structural calculations with ARIA[26] indicate the absence of organization of the aliphatic regions of the molecule (SI Figure 9a,b and Table 4).

LTB4 in the Presence of Perdeuterated BLT2. We have previously established that BLT2 folded in APols displays an affinity for LTB4 similar to that observed with the same receptor in its membrane environment[17] (SI Figure 10). To determine the structure of LTB4 bound to APol-complexed wild-type BLT2 (wtBLT2), we relied on the observation of intramolecular ^{1}H−^{1}H interactions through the dipolar cross-relaxation phenomenon[33] in a transferred mode.[34] Chemical shift variations with respect to free LTB4 are similar to those observed in the presence of DAPol alone, whereas the line broadening indicates a slow intermediate chemical exchange[35] in the presence of the receptor, in accordance with an equilibrium dissociation constant, K_d, below the micromolar range (∼200 nM) (SI Figure 8). To facilitate NOE detection and interpretation, we used perdeuterated wtBLT2 and a partially deuterated APol (DAPol). The concentration of BLT2 (17 μM) in the NMR sample being relatively low compared to that of the ligand (∼140 μM), the perdeuteration of the receptor is primarily designed to avoid any protein-mediated spin diffusion.[28] Indeed, intermolecular indirect pathways of dipolar relaxation have been shown to induce larger errors in calculated distances than intramolecular indirect pathways, an effect that is difficult to correct for when the structure of the protein is unknown or when the protein is not extensively perdeuterated. Intra-LTB4 spin diffusion was taken into account by implementing a full relaxation matrix approach[36] for analyzing transferred NOEs. This approach was preferred to the method based on the initial rates of NOE build-up[37] using the isolated spin-pair approximation, because of the low sensitivity observed at short mixing times and because of the restrictions imposed by the high affinity of the ligand. ARIA associated to CNS allows a safer structure calculation with indirect magnetization transfer corrected distances.[29] 2D NOESY experiments performed at four different τ_m (50, 100, 200, and 500 ms) gave rise to many NOE cross-peaks (Figures 1c and 2). Most strikingly, numerous cross-peaks arise between olefinic and aliphatic protons, even at short τ_m, at variance with the NOE pattern obtained in presence of the surfactant alone (Figure 3c,d).

Specificity of LTB4/BLT2 Interactions. We next assessed the specificity of the interaction between BLT2 and LTB4. As stated above, the recombinant APol-complexed receptor displays an affinity for LTB4 similar to that of BLT2 in membrane fractions.[17] However, we cannot *a priori* assert that the NOEs observed in Figure 2 reflect the structure of LTB4 bound to its specific site, given that (i) there is a 8.6 × molar excess of ligand over the receptor, and (ii) the ligand concentration is almost 3 orders of magnitude above the K_d ([LTB4] ≃ 140 μM; K_d = 169 nM[17]), raising the possibility of nonspecific binding. A competition assay by 12(*S*)-hydroxy-5*Z*,8*Z*,10*E*,14*Z*-eicosatetraenoic acid[38] (12(*S*)-HETE, Figure 3a), a ligand that specifically binds to BLT2 with a ∼10-fold lower affinity than LTB4[39] (SI Figure 10), was carried out in the presence of BLT2 at several HETE/LTB4 molar ratios, namely 1.6:1, 4.2:1, and

(34) Balaram, P.; Bothner-By, A. A.; Dadok, J. *J. Am. Chem. Soc.* **1972**, *94*, 4015–4017.
(35) Levitt, M. In *Spin Dynamics*; Wiley: Chichester, UK, 2001; pp 490−493.
(36) Keeper, J. W.; James, T. L. *J. Magn. Reson.* **1984**, *57*, 404–426.
(37) Kumar, A.; Wagner, G.; Ernst, R. R.; Wüthrich, K. *J. Am. Chem. Soc.* **1981**, *103*, 3654–3658.
(38) Hamberg, M.; Samuelsson, B. *Proc. Natl. Acad. Sci. U.S.A.* **1974**, *71*, 3400–3404.
(39) Yokomizo, T.; Kato, K.; Hagiya, H.; Izumi, T.; Shimizu, T. *J. Biol. Chem.* **2001**, *276*, 12454–12459.

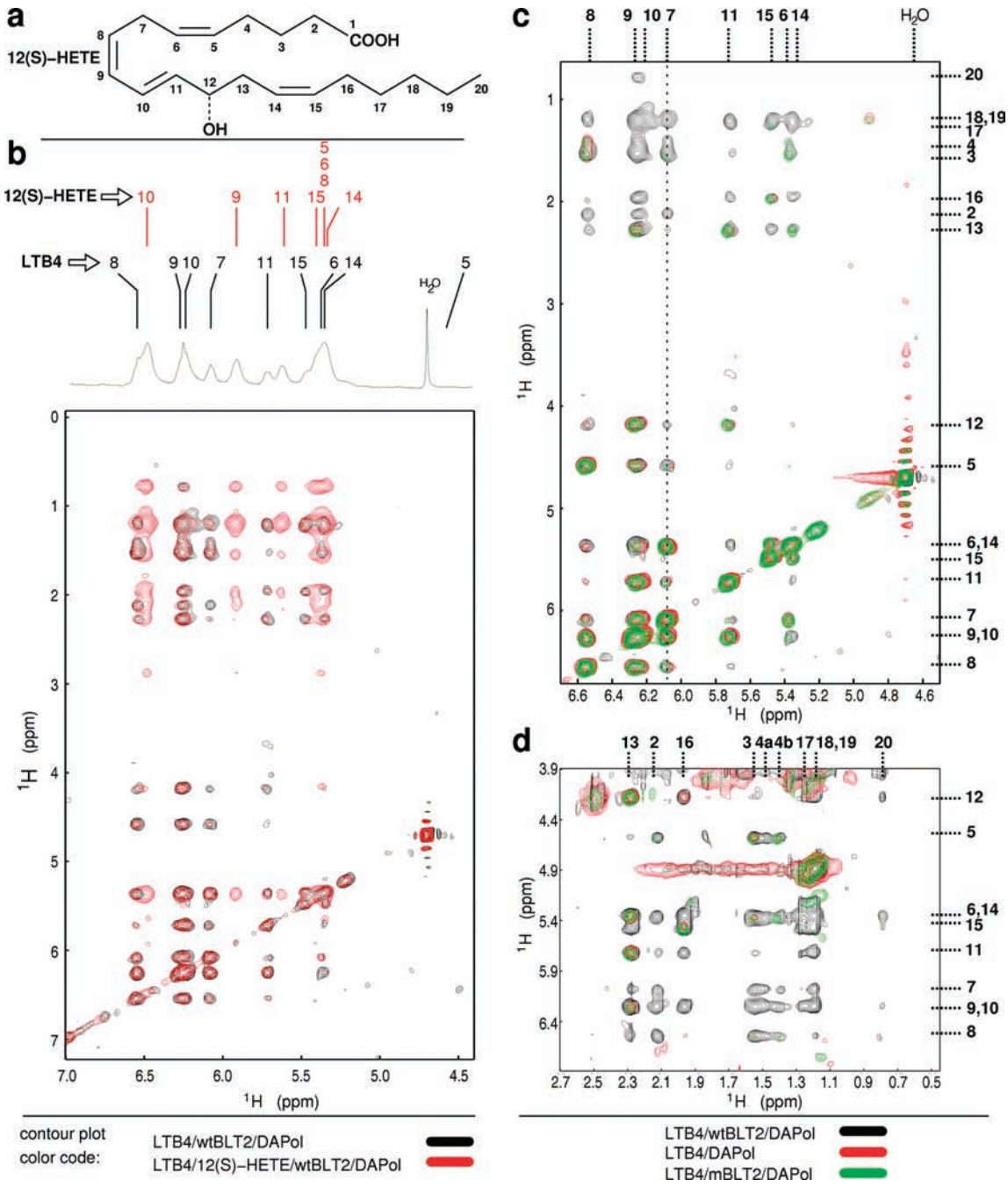

Figure 3. Control experiments. (a,b) Competitive displacement of LTB4 by 12(*S*)-HETE. (a) Chemical structure of 12(*S*)-HETE. (b) Positive contours of a 2D NOESY region of LTB4/u-^{2}H-wtBLT2/DAPol in the absence (in *black*, from Figure 2) and presence (in *red*) of 12(*S*)-HETE (molar ratio HETE/LTB4 = 9.0:1). The corresponding 1D ^{1}H spectrum of HETE/LTB4/u-^{2}H-wtBLT2/DAPol sample is shown above the 2D spectra with numbers associated to solid lines that refer to ^{1}H nucleus assignments for the two eicosanoids. (c,d) Enlarged views of two regions of 2D NOESY superimposed spectra of LTB4 in the presence of u-^{2}H-wtBLT2/DAPol complexes (from Figure 2, in *black*), u-^{2}H-mBLT2/DAPol complexes (in *green*), or DAPol alone (in *red*) (τ_m = 0.5 s, ν_H = 600 MHz, 25 °C). Numbers associated to dotted lines refer to ^{1}H nuclei of LTB4 (see Figure 1a). The dotted line over the spectra in (c) indicates the columns displayed in Figure 1. For clarity, only positive contours are plotted.

9.0:1. The structure of 12(*S*)-HETE presents enough differences with that of LTB4 to give rise to specific signals with distinct ^{1}H chemical shifts, in particular in the olefinic region (SI Figure 11). At all the HETE/LTB4 molar ratios tested, intense intra-12(*S*)-HETE NOE cross-peaks are observed in 2D NOESY spectra (Figure 3b). Conversely, LTB4 NOE cross-peak volumes decrease when the HETE/LTB4 molar ratio increases (Figure 1d and SI Figure 12), indicating that the BLT2-specific agonist 12(*S*)-HETE displaces LTB4 from its binding site on BLT2/DAPol complexes.

A second control experiment to assess the specificity of the LTB4-BLT2 interaction was carried out using a BLT2 mutant that does not specifically bind LTB4. The mutant, hereafter mBLT2, was obtained by mutating to alanines residues S135 and M136, in the third transmembrane (TM) segment of BLT2, as well as residues W268 and N275, in TM6. These residues were selected as being potentially part of the LTB4-binding pocket based on chemical cross-linking and modeling data obtained with the closely related BLT1 receptor (unpublished data). According to CD spectra and SEC profiles, mBLT2 folds

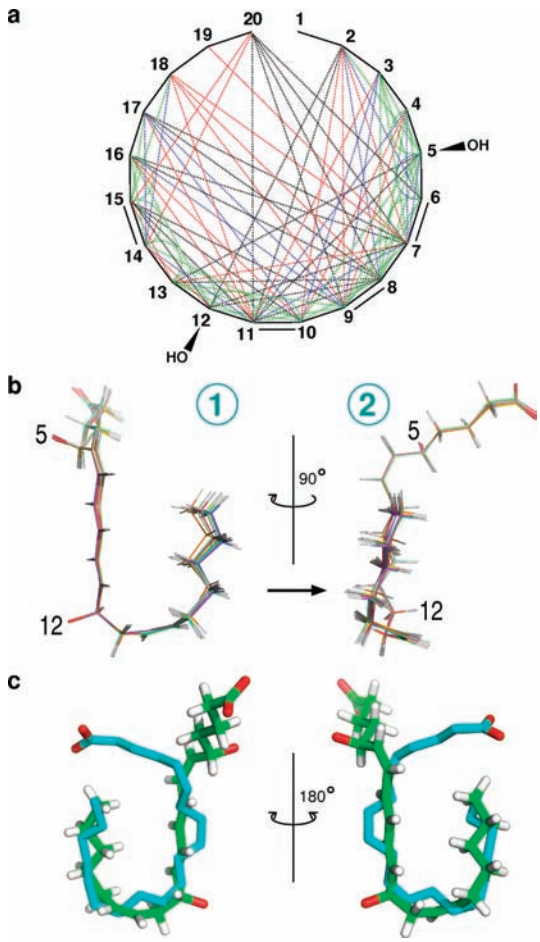

Figure 4. Three-dimensional structure of LTB4 associated to wtBLT2. (a) Experimental NOE-based distance restraints used in the structure calculation represented by dotted lines on a regular icosagon symbolizing the eicosanoid (in *green*, *blue*, *red*, and *black* distant restraints obtained with $\tau_m = 50$, 100, 200, and 500 ms, respectively. See also SI, Figure 4). (b) Two different views of an ensemble of 10 energy-minimized conformers (in *white*, hydrogen atoms; in *red*, oxygen atoms; carbon atoms are assigned a different color for each conformer). Numbers indicate the two hydroxyl groups on positions 5 and 12. (c) Superimposed structures of LTB4 (in *green*) and of arachidonic acid bound to the adipocyte lipid-binding protein (in *cyan*, from ref 51 pdb access number 1ADL). Hydrogens of the arachidonic acid have been omitted for clarity.

normally when transferred from SDS to APol, but as expected, its affinity for LTB4 is drastically diminished (see ligand-binding isotherm in SI Figure 13). A 2D NOESY experiment of the LTB4/mBLT2/DAPol sample gives rise to a spectrum almost identical to that obtained with the LTB4/DAPol sample (Figure 1e and Figure 3c,d). Importantly, almost none of the cross-peaks involve aliphatic protons located at either end of the molecule, in contrast to what is observed with the wild-type receptor.

Taken together, these two control experiments strongly support the view that intramolecular $^1H-^1H$ interactions observed through the transferred dipolar cross-relaxation effect in the presence of wtBLT2 reflect the conformation of LTB4 bound onto its specific, physiologically relevant binding site.

Structure of LTB4 Bound to Human BLT2. The 2D NOESY experiments yielded 89 NOE-based distance restraints (Figure 4a and Table 1), from which the structure of LTB4 was calculated using ARIA. On the whole, the ensemble of converged structures depicts a highly constrained LTB4 molecule, adopting a seahorse conformation (Figure 4b and SI Figures 14 and 15). Starting from the terminal methyl group,

Table 1. Summary of Structural Constraints and Structure Statistics for a Set of 100 Structures (Unless Otherwise Indicated)

NOE-Based Distance Restraints	
interprotons *i*,*j*	
$\|i-j\| = 1$	11
$\|i-j\| = 2$	14
$\|i-j\| = 3$	10
$\|i-j\| = 4$	11
$\|i-j\| = 5$	9
$\|i-j\| = 6$	9
$\|i-j\| = 7$	7
$\|i-j\| = 8$	5
$\|i-j\| = 9$	5
$\|i-j\| = 10$	3
$\|i-j\| = 11$	2
$\|i-j\| = 12$	2
$\|i-j\| = 13$	1
$\|i-j\| = 14$	1
total	89
Structural Statistics	
number of NOE violations >0.1 Å	0
mean rms NOE (Å)	$4.7 \times 10^{-3} \pm 9.1 \times 10^{-4}$
mean global rms (Å)	0.36 ± 0.16
mean global rms/10 structures (Å)	0.13 ± 0.05
Deviation from Idealized Geometry	
mean rms bond (Å)	$4.5 \times 10^{-3} \pm 9.3 \times 10^{-5}$
mean rms angle (deg)	$0.90 \pm 4.5 \times 10^{-3}$
mean rms improper (deg)	$1.55 \pm 7.2 \times 10^{-3}$
mean rms dihedral (deg)	$0.65 \pm 5.8 \times 10^{-3}$
Mean Energies (kcal·mol^{-1})	
E_{bonds}	$1.06 \pm 4.38 \times 10^{-2}$
E_{angles}	11.39 ± 0.11
$E_{impropers}$	11.03 ± 0.10
$E_{dihedrals}$	$3.53 \pm 6.16 \times 10^{-2}$
E_{vdw}	-11.26 ± 0.48
E_{total}	15.76 ± 0.46

the structure can be divided into three regions: from carbon atoms 20 to 15, a tail folding back along an elongated trunk (carbons 14 to 6), and a head bent almost at right angle to the body (carbons 5 to 1). Globally, carbons 6−13 and 16−20 are roughly in the same plane (Figure 4b, view 2), the early part of the chain being oriented nearly perpendicular to it.

Because most putative interaliphatic $^1H-^1H$ NOEs are masked by signals from the surfactant, the structure is more loosely defined at both extremities, especially between carbons 1 and 4 (see SI, Figure 14). This precludes any conclusion about the mobility of this part of the molecule as compared to that of the rest of the skeleton. Nonetheless, several important features can be deduced from the data. First, the ensemble of converged structure (SI Figure 14) suggests that, at variance with that of LTB4 free in solution,[32] the triene motif is not planar. The distribution of the dihedral angle ζ (Figure 1a) over 100 conformers indicates a highest probability for the double bond H6−C6−C7−H7 to be slightly tilted away from the plane defined by the two other conjugated double bonds (see SI, Figure 16a). Second, in the same region of the molecule, associated to the deformation of the triene, there is a steric interaction between H5 and H8, characterized experimentally by a strong NOE. At variance with the distortion of the triene, this steric interaction has already been described for LTB4 free in solution, which, as regards the rotation about the C5−C6 bond, adopts preferentially an eclipsed conformation in which H5 and H6 are in trans conformation.[32]

Another striking characteristic of the structure of LTB4 in its BLT2-bound state is the tail folding back along the triene motif, as revealed by the many NOEs observed between protons

H7−H11 and protons H16−H20 (Figures 2 and 4a). Its conformation causes two additionnal proton−proton steric interactions not observed in solution, namely one proton H13 interacting with H11 on one side and with one H16 proton on the other. The seahorse fold renders fully accessible the hydroxyl group connected to C12, the C12−OH bond being almost perpendicular to the plane defined by carbons C7−C12. This is close to the preferred conformation (populated to ∼60%) found in the free state, where C11−C12 and H12 were described to be in the same plane as the rest of the triene.[32] On the other hand, the dihedral angle λ (see Figure 1a) corresponds more or less to an eclipsed conformation (SI Figure 16c) that is not observed in the free state (which features two equally populated rotamers with OH or C6 bisecting H13a and H13b[32]), while the rotations about C13−C14 and C15−C16, represented by three equally populated rotamers in the free state, are fixed in the bound one. The remaining carbon atoms C15−C20, like C1−C4, are all in a trans conformation, except for C18 with respect to C15 (SI Figure 16d).

Discussion

Ligand binding is the first step of signal transduction through GPCRs. Identifying the molecular bases of ligand recognition by these receptors is therefore crucial to understanding the way a receptor is activated by its agonist. It is also important for designing specific drugs for pharmacological purposes. To date, however, structural information about GPCR ligands bound to their receptors is rare. The most detailed information available concerns the ligands present in some of the receptor crystal structures obtained so far,[2−5,7] in addition to a handful of NMR studies.[40−43] NMR spectroscopy can be quite powerful to investigate ligand-specific conformational changes of GPCRs, as recently demonstrated with the β_2 adrenergic receptor.[8] We have used it to study the conformation adopted by the LTB4 agonist upon binding to its BLT2 receptor. Our data provide direct experimental evidence that this conformation differs very markedly from those populated in solution. In other words, it is strongly constrained by its proteic environment. Besides the interest of such a result from a pharmacological perspective, the present work demonstrates that solution NMR experiments can provide detailed information about the interaction of ligands with receptors for which structural data at the atomic level are currently lacking.

The approach we have resorted to depends on the production of a recombinant receptor in sufficient yield. In this context, the procedure we recently described, which relies on the folding in APols of receptors recovered from bacterial inclusion bodies, appears as a highly favorable step.[17] This method is not specific to BLT2[17] nor to GPCRs.[44] With a stable, purified, functional receptor, NMR spectroscopy becomes particularly suitable to investigating the structure of a bound ligand through the dipole-to-dipole cross-relaxation phenomenon. Moreover, given favorable kinetics, NOEs can be collected in a transferred mode, even with a K_d below the micromolar range.[30,45] Such an approach has the great advantages of making it possible to work at low receptor concentrations (<20 μM) and of not being limited by the size of the MP/APol complexes.

The interpretation of NMR experiments carried out well above the K_d of the ligand is far from trivial given the number of potential sites for nonspecific binding (Figure 1). Nevertheless, control experiments show that the NOE signals collected do correspond to a specific interaction. (i) Distinct NOE signals are observed in the presence of wild-type BLT2 compared to those observed with free LTB4 solutions, or when LTB4 is added either to DAPol alone or to complexes between DAPol and a mutant BLT2 (mBLT2) that does not bind LTB4 (Figure 1). (ii) Only in the presence of the wild-type receptor are numerous NOEs observed, including many cross-peaks between olefinic and aliphatic LTB4 protons, the analysis of which gives rise to a converging ensemble of well-constrained structures (Figure 4b and SI Figure 14). On the contrary, with the exception of interactions of olefinic protons between themselves and with protons H5 or H12, very few NOEs can be observed even at long mixing times for LTB4/DAPol and LTB4/mBLT2/DAPol mixtures (Figure 3c,d). Structure calculations confirm the absence of organization of the aliphatic parts of the eicosanoid in the absence of wtBLT2 (SI Figure 9). (iii) A competition experiment, using the BLT2-specific eicosanoid 12(*S*)-HETE to displace LTB4, reveals strong interactions of this BLT2 agonist with wtBLT2, accompanied by a decrease of the LTB4 NOE cross-peak signals between olefinic and aliphatic protons (Figure 1e and SI Figure 12).

LTB4 undergoes a significant conformational adaptation upon binding to the BLT2 receptor. In contrast to what is observed with free LTB4 in solution, interdipolar ^{1}H−^{1}H distances deduced from NOE measurements indeed lead to an convergent ensemble of highly constrained structures, the seahorse conformation. The narrow distribution of LTB4 structures obtained should be considered with some caution, due to the method used to handle spin diffusion in the analysis of NOEs (see Material and Methods section). In other words, the strong convergence observed may be partially a consequence of the method of analysis. At long mixing time, considering a lifetime of the bound state, τ_b, of ∼50 ms (*vide infra* the rough estimation of k_{off}), the amount of free ligand that has interacted with the receptor increases, compared to short τ_m values. This can give rise to stronger NOEs that could be misinterpreted as spin diffusion in the treatment with the complete relaxation matrix. Nonetheless, performing a structure calculation with only those data collected at the two longest mixing times (200 and 500 ms, i.e. well above τ_b) leads to a set of structures equivalent to that obtained with the four sets of NOE signals (from 50 to 500 ms; not shown), suggesting that the lag time (e.g., see ref 46) does not have much impact on the NOE-derived distances. Furthermore, back calculations with TRNOE[30] indicated that NOE evolutions with mixing time are consistent with the estimated off-rate constant k_{off} of 20 s^{-1} (for a comparison, see SI Figure 5).

The complexities associated with properly taking care of spin diffusion effects as well as of some contributions from nonspecific binding do not prevent the emergence of two

(40) Inooka, H.; Ohtaki, T.; Kitahara, O.; Ikegami, T.; Endo, S.; Kitada, C.; Ogi, K.; Onda, H.; Fujino, M.; Shirakawa, M. *Nat. Struct. Biol.* **2001**, *8*, 161–165.
(41) Lopez, J. J.; Shukla, A. K.; Reinhart, C.; Schwalbe, H.; Michel, H.; Glaubitz, C. *Angew. Chem., Int. Ed.* **2008**, *47*, 1668–1671.
(42) Kofuku, Y.; Yoshiura, C.; Ueda, T.; Terasawa, H.; Hirai, T.; Tominaga, S.; Hirose, M.; Maeda, Y.; Takahashi, H.; Terashima, Y.; Matsushima, K.; Shimada, I. *J. Biol. Chem.* **2009**, *284*, 35240–35250.
(43) Yoshiura, C.; Kofuku, Y.; Ueda, T.; Mase, Y.; Yokogawa, M.; Osawa, M.; Terashima, Y.; Matsushima, K.; Shimada, I. *J. Am. Chem. Soc.* **2010**, *132*, 6768–6777.
(44) Pocanschi, C. L.; Dahmane, T.; Gohon, Y.; Rappaport, F.; Apell, H. J.; Kleinschmidt, J. H.; Popot, J.-L. *Biochemistry* **2006**, *45*, 13954–13961.
(45) Williamson, M. P. In *Modern Magnetic Resonance*; Craik, D., Ed.; Kluwer Academic Press: Netherlands, 2006; pp 1339−1344.
(46) Campbell, A. P.; Sykes, B. D. *Annu. Rev. Biophys. Biomol. Struct.* **1993**, *22*, 99–122.

noticeable structural features of BLT2-bound LTB4: a warped triene plane and a tail that folds back along the triene motif. The latter feature strongly differs from two models of LTB4 bound to the BLT1 receptor,[47,48] which have the tail extending in the opposite direction. We previously proposed, on the basis of circular dichroism data obtained with the purified BLT1 receptor, that a torsion of the triene occurs upon binding to the receptor.[49] Even though the structure of LTB4 obtained here appears loosely defined in some part of the molecule (SI. Figure 14), the data presented do suggest a twisted conformation of LTB4 when bound to BLT2. Model calculations show that even a modest deviation from planarity, like that observed in the present study (highest probability $\simeq$10°), can have intense effects on CD spectra.[49,50] Globally, except for the orientation of the head, the seahorse fold has already been observed with another eicosanoid, arachidonic acid, bound to the adipocyte lipid-binding protein[51] (Figure 4c). One consequence of LTB4 adopting the seahorse conformation is to make both OH groups accessible for interacting with amino acids of the binding site. In the case of BLT2, the hydroxyl group in position 5 (OH(5)) is thought not to be crucial for the binding of the eicosanoid to the receptor.[52] Indeed, 12(*S*)-HETE, which does not feature OH(5), is one of the ligands with the most affinity for BLT2, while it does not bind to BLT1.[39]

In the absence of G proteins, the specific interaction between LTB4 and BLT2 observed in this study corresponds to the low-affinity state of the uncoupled receptor (K_d of $\sim$200 nM). Observing transferred NOEs for ligands whose equilibrium dissociation constant is submicromolar is not exceptional (see e.g. ref 45). Given that we do observe transferred NOEs, the k_{off} of LTB4 from BLT2 must be high enough with respect to the spin−lattice relaxation rates and the mixing times we used. It implies a correspondingly fast rate of association, such as a diffusion-controlled k_{on}.[53] For a K_d of $\sim$200 nM, these conditions are met, for instance, by the combination of a k_{off} of $\sim$20 s^{-1} and a k_{on} of $\sim 10^8$ $M^{-1}\cdot s^{-1}$. One may also note that, even though the ligand is fully protonated, the dilution of the ^{1}H thermal bath caused by the perdeuteration of the receptor reduces substantially the ^{1}H longitudinal relaxation rates in the complex, making the observation of transferred NOE easier.

It seems probable that further conformational changes take place during the low-to-high affinity switch observed in the presence of G-proteins. It is also to be noted that the refolded BLT2 receptor is essentially dimeric under the conditions used (see Figure 6 in ref 17). The purified dimeric receptor in the absence of G proteins displays a single class of LTB4-binding sites, with no evidence for cooperativity effects (ref 17 and unpublished observations). The identity of the two dissociation constants in the dimer and the convergence of the NOE-derived LTB4 structures strongly suggest that both the binding site and the ligand adopt the same structure in the two protomers. The structure inferred from our NMR experiments likely represents that of LTB4 bound to one or the other of the two protomers in the dimeric receptor. In a tentative model of the orientation of LTB4 in the binding site, OH(5) would rather be oriented toward the extracellular loops of the protein. *A contrario*, OH(12), which is thought to be indispensable to the binding to either the BLT1 or BLT2 receptors,[52] would face the bottom of the pocket.

The seahorse conformation, at variance with elongated conformations, is not significantly populated in solution.[32] In other words, this fold results from strong constraints applied by amino acids residues lining the binding pocket. In particular, two steric interactions involving one H13 proton (with H11 and one H16 proton) render the LTB4 architecture highly dependent on the local organization of the helices of BLT2. Conversely, such strains are likely to modulate the equilibrium between conformational states of the receptor, as qualitatively observed by NMR (SI Figure 17). From a more general perspective, our observations are consistent with the view that a clear understanding of the active structure of a ligand can only be inferred from a structural analysis carried out in the presence of its cognate receptor. In this context, the approach described here, based on both an efficient procedure for producing a functional isolated receptor in high yield and an NMR-based analysis of the structure of the ligand in its GPCR-bound state, appears particularly powerful and could significantly contribute to a detailed analysis of the molecular events that lead to receptor activation and therefore signaling.

Acknowledgment. We are extremely grateful to Yasmine Chebaro (UPR 9080 CNRS, IBPC, Paris) for assistance with AMBER software, and Benjamin Bardiaux and Thérèse Malliavin (URA 1129 CNRS, Institut Pasteur, Paris) for support and information concerning the software ARIA. We express our gratitude to Marie-Noëlle Rager (ChimieParisTech, Paris) and Hervé This and Audrey Tardieu (UMR 214 INRA, AgroParisTech, Paris) for accesses, respectively, to Avance Bruker 400 and 300 MHz spectrometers to perform early tests with eicosanoids. Special thanks are due to François Bontems and Ewen Lescop (ICSN, Gif/Yvette), and Jacky Marie and Sophie Mary (IBMM, Montpellier) for helpful discussions. This work was supported by the Centre National de la Recherche Scientifique (CNRS), Paris-7 University, and by grants from the E.U. (Specific Targeted Research Project LSHG-CT-2005-513770 IMPS Innovative tools for membrane protein structural proteomics) and from the French Ministry of Research (ANR-06-BLAN-0087 and ANR BLAN07-1/_191475). LJC is a 2009 recipient of *Projets Exploratoires/Premier Soutien* (PEPS, *Leukomotive* project) from the CNRS.

Supporting Information Available: Complete refs 8 and 19. DAPol chemical structure, time-dependent stability of A8-35-folded BLT2 at 25 °C, COSY spectra of LTB4 free in solution, the four sets of NOE data used in the structure calculation, experimental and simulated evolution of the intensity of transferred-NOE cross-peaks as a function of the off-rate dissociation constant and mixing time, a comparative evolution of the NOE cross-peak volume with the mixing time for LTB4 in presence of wtBLT2/DAPol, mBLT2/DAPol, or DAPol only in solution, two one-dimensional ^{1}H superimposed spectra of LTB4 free in solution or in the presence of DAPol only, olefinic ^{1}H NMR spectra of LTB4 in different environments, the three-dimensional structure of LTB4 interacting with DAPol particles and in the presence of mutant BLT2/DAPol complexes, the

(47) Sabirsh, A.; Bywater, R. P.; Bristulf, J.; Owman, C.; Haeggström, J. Z. *Biochemistry* **2006**, *45*, 5733–5744.
(48) Basu, S.; Jala, V. R.; Mathis, S.; Rajagopal, S. T.; Del Prete, A.; Maturu, P.; Trent, J. O.; Haribabu, B. *J. Biol. Chem.* **2007**, *282*, 10005–10017.
(49) Baneres, J.-L.; Martin, A.; Hullot, P.; Girard, J. P.; Rossi, J. C.; Parello, J. *J. Mol. Biol.* **2003**, *329*, 801–814.
(50) Weiss, U.; Ziffer, H.; Charney, E. *Tetrahedron* **1965**, *21*, 3105–3120.
(51) LaLonde, J. M.; Levenson, M. A.; Roe, J. J.; Bernlohr, D. A.; Banaszak, L. J. *J. Biol. Chem.* **1994**, *269*, 25339–25347.
(52) Leblanc, Y.; Fitzsimmons, B. J.; Charleson, S.; Alexander, P.; Evans, J. F.; Rokach, J. *Prostaglandins* **1987**, *33*, 617–625.
(53) Gabdoulline, R. R.; Wade, R. C. *Cur. Opin. Struct. Biol.* **2002**, *12*, 204–213.

pharmacological profile of A8-35-folded BLT2, a zoom on the olefinic region of two one-dimensional ^{1}H superimposed spectra of LTB4 and 12(*S*)-HETE, illustrations of the competition experiment with the 12(*S*)-HETE eicosanoid, binding of LTB4 to wild-type BLT2 (wtBLT2) and mutant BLT2 (mBLT2) receptors, views of an ensemble of 100 energy-minimized conformers of LTB4 associated to wild-type BLT2 receptor, stereoscopic view of one LTB4 conformer, analysis of dihedral angles on an ensemble of 100 structures, comparative [^{15}N,^{1}H] CRINEPT spectra of wild-type [^{2}H,^{15}N] BLT2 in complex with DAPol before and after addition of LTB4, tables of LTB4 ^{1}H chemical shifts and structural constraints and structure statistics for LTB4 in the presence of DAPol only or mutant receptor, NOESY experiment of LTB4 free in solution, intra-aliphatic LTB4 correlations, and associated references. This material is available free of charge via the Internet at http://pubs.acs.org.

JA101868C